Online correction of aberrations to reduce the measuring uncertainty for the optical high-speed measurement of high-precision cutting tools using coordinate measuring machines

Marco Büchner[1], Silvio Holder[2], Frank Richter[1] and Dr. Uwe Nehse[1]

[1]Mahr OKM GmbH, Jena, Germany
[2]Faculty of Mechanical Engineering, Department of Quality Management, Ilmenau, Germany

Abstract – This paper presents a novel approach to correct aberrations, especial the telecentricity error of lenses during the optical measurement of high-precision cutting tools. The displacement of the cutting edges from the focus plane because of the high-speed measuring process is determined based on focus methods and the 4D axis information from the coordinate measuring machine. The known displacement and the offline determined correction function to describe the telecentricity error of lenses are used for the online correction of each measurement point. So the measuring uncertainty because of the increasing influences of aberrations during the high-speed acquisition process can be reduced.

Keywords aberrations, correction, tool measurement

1. INTRODUCTION

The trends in industrial engineering lead to new and increasing demands of production metrology [1]. One trend is the 100% inspection. This is also the aim in precision tool manufacturing. But most methods for visual inspection of high-precision cutting tools do not achieve the increasing demands. In [2-4] new dynamic measuring methods to reduce the measuring time, which is one increasing demand [1], are presented. The reduction of measuring time increases the operating grade of coordinate measuring machines (CMM). The disadvantage of the dynamic measuring methods in contrast to static measuring methods [5] is the increasing influence by aberrations, which directly increase the measuring uncertainty and the measurement accuracy. In [4] the measuring uncertainty is reduced by decreasing the angle resolution during the acquisition process at the expense of the measuring time. In this paper a novel approach to reduce the measuring uncertainty by the online correction of aberrations is presented. Distortion [6-8] and telecentricity error [9] of optical systems are the most influential errors. Whereas the correction of distortion is state of the art, the error of inaccurate telecentricity is usually considered by the optical design and the measurement setup. For this reason this paper is focused on the correction of the telecentricity error of lenses during the measuring process.

2. THEORY AND METHOD

2.1. Basics

Based on an object side telecentric imaging "Fig. 1", the telecentricity error τ is defined according to "(1)".

$$\tau = \frac{\Delta W}{\Delta z} = \frac{W_2 - W_0}{z_2 - z_0} \qquad (1)$$

By changing the object distance Δz within depth of focus an apparent change ΔW of the object size W_0 occures. Inside the telecentric range T is not a measurement relevant alteration [10]. Including the image scale "(2)", it can be shown that the result for the correction of the telecentricity error is a distance depending change of the image scale.

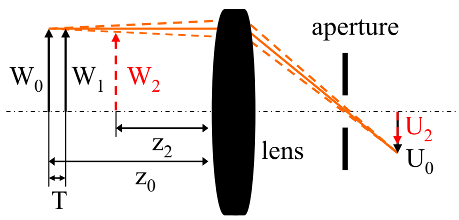

Fig. 1 Object side telecentric imaging with apparent resizing of the object W_0 because of the telecentricity error

For a known object size W_0 the telecentricity error respectively the changing of the image scale can be determined according to "(3)" by changing the object distance z [10].

$$W_0 = \frac{U_0}{\beta_0} = U_0 \cdot \omega_0 \qquad (2)$$

Based on "(3)" a function $\omega_z = f(z)$ can be determined, which is described in section 2.1. Therefore ω_z and ω_0 are known and single measuring points or complete measuring results can be corrected online during the measurement according to "(4)".

$$\omega_z = \frac{U_0}{U_z} \cdot \omega_0 = \frac{W_0}{W_z} \cdot \omega_0 \qquad (3)$$

$$W_z^{corr} = \frac{\omega_z}{\omega_0} \cdot W_z \qquad (4)$$

2.2. Calibration

In case of CMM's it is possible to realize a defined changing of the object distance easily by positioning the sensor or the object along the optical axis. This is the basic of the calibration. For the determination of function $\omega_z = f(\Delta z)$ to describe the telecentricity error of lenses, an optical ball plate with defined circles "Fig. 2" is used. The same template can also be used for the distortion calibration [6].

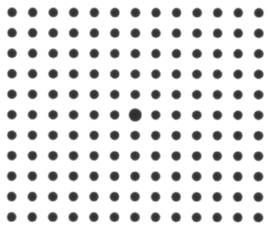

Fig. 2 Optical ball plate to determine the telecentricity error of lenses

All the circles on the template are measured in different displacements from the focus plane and the distances of the circle center points to the calibration values "Fig. 3" are used to calculate ω_z for each point separated in the u and v coordinate of the 2D image plane according to "(3)". The circle center point in the center of image plane is the origin of the coordinate system.

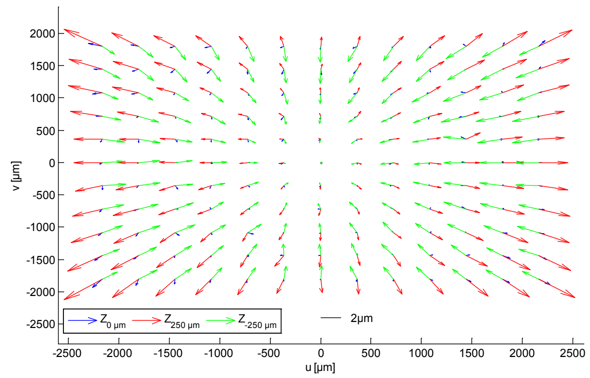

Fig. 3 2D deviations between a nominal grid (circle center points of the optical ball plate) with known distances and the measured distances for different displacements (-250µm, 0µm, 250µm) from the focus plane.

The mean value over the rows and columns is calculated to simplify the algorithm and to get one representation of the image scale for u and v according to "(5)".

$$\omega_z^u = \frac{1}{N} \cdot \sum_{i=1}^{N} \omega_z^{u^i} \; ; \omega_z^v = \frac{1}{M} \cdot \sum_{j=1}^{M} \omega_z^{v^j} \qquad (5)$$

The resulting curves for ω_z^u and ω_z^v of the applied 1.5x zoom lens are shown in "Fig. 4". You can see that the changes are nearly linear. For the approximation of ω_z^u and ω_z^v a two linear equations model is used according to "(6)". The coefficients in "(6)" are determined by least squares estimation.

$$\omega_z = f(\Delta z) = \begin{cases} a_1 \cdot \Delta z + n_1, & \Delta z \le 0 \\ a_2 \cdot \Delta z + n_2, & \Delta z > 0 \end{cases} \qquad (6)$$

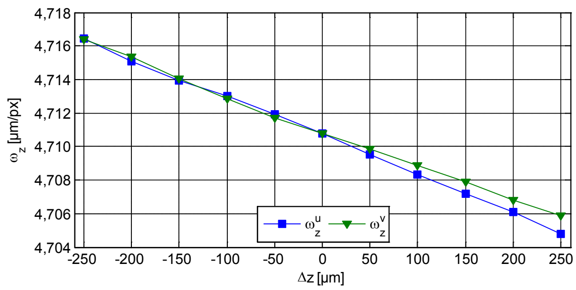

Fig. 4 Changes of the image scale depending of the displacement from the focus plane

2.3. Online Correction

Because of the high-speed acquisition process within the inspection method of cutting tools [4], called dynamic contour scan (DCS), the maximum error C_e^{max} in the angle "(7)" and the maximum error of the tool radius "(8)" depending on the angle resolution A is introduced in [4]. The high-speed acquisition process bases on recording sequences of images and 4D machine positions during rotating the cutting tool, where C_i are the recorded information of the rotation axis and N_i the corresponding images. The error in the angle for a region of interest (ROI) can be calculated according to "(9)".

$$C_e^{max} = \frac{1}{2}(C_{i+1} - C_i) = \frac{1}{2} A \qquad (7)$$

$$dRf^{max} = R(1 - \cos(C_e^{max})) \qquad (8)$$

$$C_e = \begin{cases} -|C_F - C_i|, & |C_F - C_i| \le |C_{i+1} - C_F| \\ +|C_{i+1} - C_F|, & |C_F - C_i| > |C_{i+1} - C_F| \end{cases} \qquad (9)$$

ROI's are used, because the cutting edges of tools are drilled. The dimensions of the ROI depend on the depth from focus and the edge geometry of the cutting tool. Therefore the whole cutting edge can not be sharp imaged, see "Fig 5". The optimum angle C_F, where the cutting edge is ideal focused inside the ROI, is determined based on depth from focus methods [11] and shown in "Fig 6". The contour of the cutting edge is determined by an edge detection algorithm within the image N_i close to the depth from focus "Fig 7".

Fig. 5 Optical imaging of drilled cutting edge ideal focused inside the region of interest ROI (red rectangle)

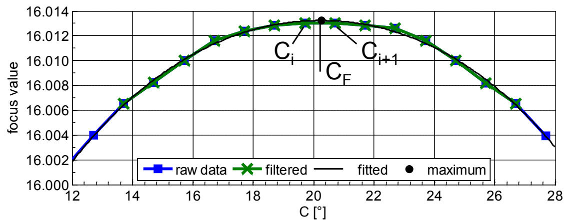

Fig. 6 Depth from focus detection for a cutting edge inside a ROI "Fig 5" by rotation the cutting tool

For sharp relief-grinded cutting edges the faulty detected contour points can be corrected by using "(9)", "(10)", "(6)" and "(4)". But the problem is, that the tool radius is unknown. Therefore the faulty measured radius R_M is used. It can be seen "(11)" that for small angle differences $\Delta\phi$ the measured radius is approximately equal to the tool radius. So the displacement Δz of the cutting edge from the focus plane within the ROI can be determined. The error in the displacement, because of the faulty determined radius R_M, is negligible.

$$\begin{aligned} \Delta\phi &= C_e \\ \Delta z &= R \cdot \sin(\Delta\phi) \end{aligned} \tag{10}$$

$$\begin{aligned} \Delta z &= \Delta z_M \\ \Delta z &= (R_M + dRf) \cdot \sin(\Delta\phi) \\ 0 &= R_M \cdot \tan(\Delta\varphi) - R \cdot \sin(\Delta\phi) \\ R &\approx R_M \end{aligned} \tag{11}$$

The complete integration of the correction algorithm into the dynamic high-speed measurement process [4] is shown in "Fig 7". For each ROI the necessary parameters are determined and all the detected contour points within the ROI are corrected depending on the lateral location of the cutting edge inside the visible field of view.

3. EXPERIMENTAL RESULTS

The verification of the correction algorithm is divided into three steps. First the optical ball plate "Fig. 2", which is used for calibration, is taken. All the circles in different displacements are measured again and corrected with the known displacement according to "(6)" and "(4)". The differences to the nominal distances after the correction are shown in "Fig. 8". In contrast to "Fig. 3" you can see that telecentricity error of the applied 1.5x zoom lens is clearly corrected. The remains of deviations in "Fig. 8" are caused by the uncorrected distortion. If you use the deviations at $\Delta Z = 0$ for distortion correction, the deviation at $\Delta Z \neq 0$ are less then 0.5µm. By using the optical ball plate a factor of the correction of four times is reached.

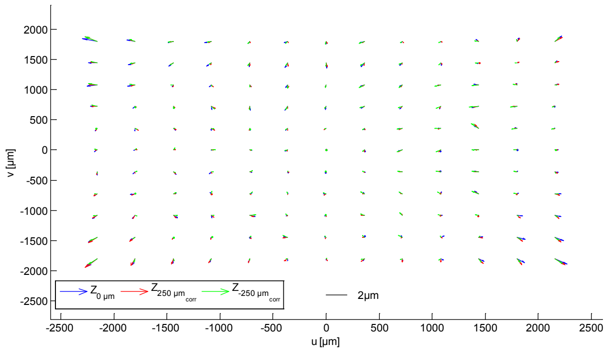

Fig. 8 2D deviations after the telecentricity error correction between a nominal grid (circle center points of the optical ball plate) with known distances and the measured distances for different displacements (-250µm, 0µm, 250µm) from the focus plane

In the next step the correction algorithm is verified by measuring the radius on one cutting edge of different cutting tools by using one ROI similar to the complex tool measurement process [4]. The cutting edge is located on different locations (top, center and bottom) inside the camera's field of view.

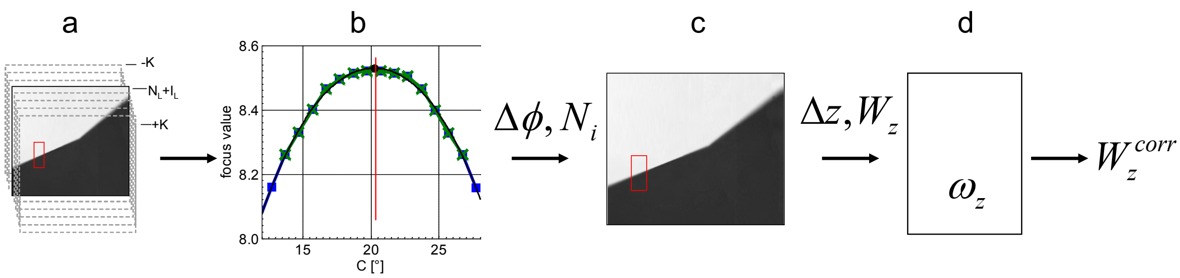

Fig. 7 Integrating the correction algorithm (d) of the location depending aberrations into the measurement process of cutting tools [4] consisting of an image acquisition process (a), depth from focus detection (b) and edge detection (c)

The optimum angle C_F for the ROI is determined in the center location, where the origin of the field of view is defined. At this location the aberrations have no influence. From the known optimum angle C_F the cutting edge is displaced from the focus plane by rotating the cutting tool in defined steps $\Delta\phi$. At every step the tool radius is measured and corrected according to "(11)", "(10)", "(6)" and "(4)". Than the differences of the measured radius and the corrected radius to the radius measured in the center are calculated. In "Fig. 9" and "Fig. 10" the results for two different cutting tools are shown.

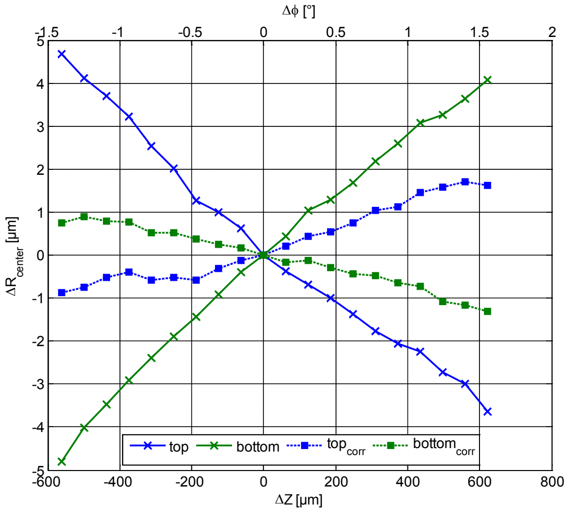

Fig. 9 Deviations of the tool radius for a blade wheel (R=28.5mm) measured and corrected at the top and bottom of the field of view to the radius measured in the origin.

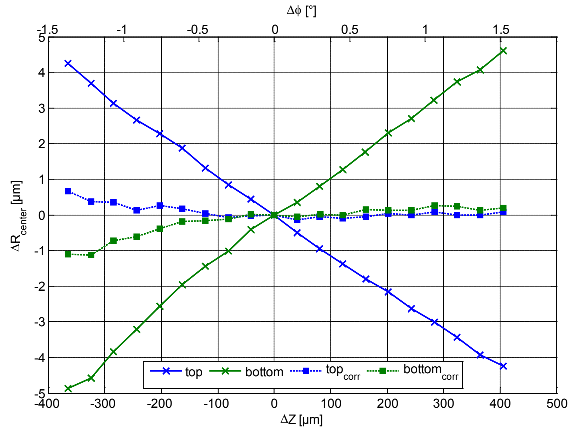

Fig. 10 Deviations of the tool radius for a fir tree cutter (R=18.6mm) measured and corrected at the top and bottom of the field of view to the radius measured in the origin.

It can be seen that it is also possible to correct the influences of the telecentricity error of the applied 1.5x zoom lens by the measurement of cutting edges. But the geometry of the cutting edge itself has a considerable influence. The results of the correction of sharp relief-grinded cutting edges are very well, c.f. "Fig. 10". The influences of the telecentricity error can be corrected less then 1µm just like the optical ball plate. At less sharpened cutting edges "Fig. 9" the residual error is greater. The factor for a possible correction is reduced to two till three times depending on the geometry of the cutting edge. In "Fig. 10" you can see that the correction results for displacements above the focus plane are very well, less then 0.5µm. Below the focus plane it seems the linear model "(6)" is not suitable enough. The reasons are the optical effects at the cutting edge and the field curvature of lenses.

In the last step the correction algorithm is integrated into the complex high-speed measuring process "Fig. 7". The aim is to reduce the measurement uncertainty for a relative high angle resolution during the acquisition [4]. Therefore it is possible to reduce the measuring time further for nearly the same uncertainty. The form deviation, which is very important for root cutters e.g. fir tree cutters, for different angle resolutions with and without correction can be seen in "Fig. 11" and "Fig. 12". In direction the results show that it is possible to reduce the faulty form deviation for an angle resolution greater than one degree. But for some points the correction is done in wrong direction. The reason is the wrong detection of the optimum focus angle C_F. Therefore it is absolutely necessary to stabilize the focus angle detection.

4. CONCLUSION AND FURTHER WORK

In this paper a novel approach to correct the influences of the telecentricity error of lenses by measuring cutting tools is proposed. First the telecentricity error is calibrated in an offline step by using a linear model to describe it. In the complex measurement process of cutting tools an algorithm for the correction of the telecentricity error to reduce the measurement uncertainty is proposed. The results show that the approach is well suited for sharp relief-grinded cutting edges like cutters. This allows the reduction of the measurement deviation and uncertainty for high-speed measurement of this kind of cutting tools. For circular-grinded cutting edges like drills and reamers the current algorithm will not be sufficient, because the assumptions "(8)" and "(11)" are not fulfilled. It has to be investigated how far the correction algorithm is applied to other optical systems, e.g. other magnifications and aberrations like the field curvature of lenses. It is conceivable to extent the correction algorithm from the linear model to a 3D-surface approach as a trilinear interpolation or a description of the image error by a volume model. For the practical use the stability of the optimum focus angle detection, which is the basis of the online correction, has to be improved.

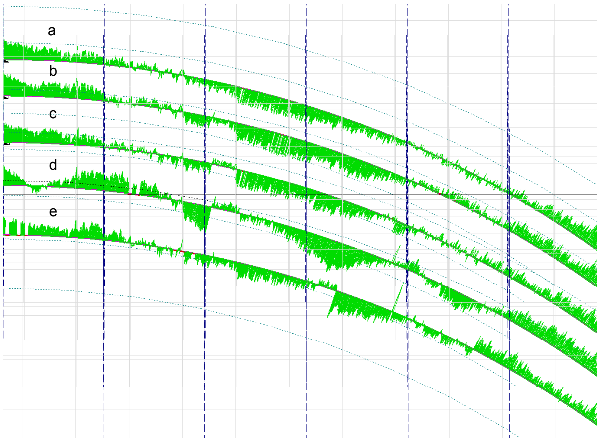

Fig. 11 Form deviations by measuring a ball end milling cutter (R=12mm) for different angle resolutions with and without telecentricity error correction, DCS 0.25° (a), DCS 1° (b), DCS 1° error corrected (c), DCS 2° (d), DCS 2° error corrected (e)

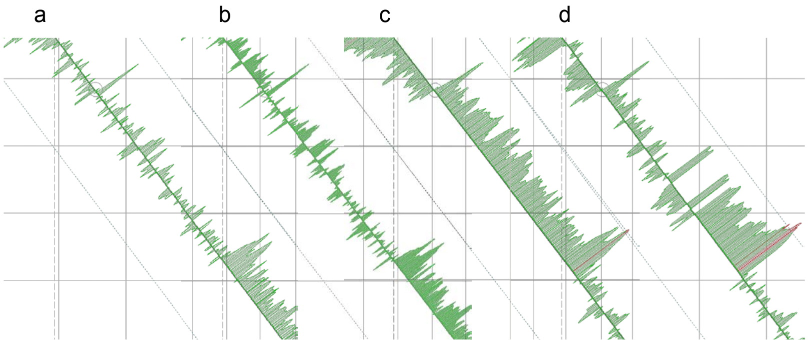

Fig. 12 Form deviations by measuring a fir tree cutter (R=13mm) for different angle resolutions with and without telecentricity error correction, static (a), DCS 0.25° (b), DCS 2° (c), DCS 2° error corrected (d)

AKNOWLEDGEMENTS

This work is encouraged by funds of the Free State of Thuringia and the European Regional Development Funds ERDF (2008 FE 9121, 2008 FE9126).

REFERENCES

[1] VDI/VDE-Gesellschaft Mess- und Automatisierungstechnik (GMA), *Fertigungsmesstechnik 2020*, Verein Deutscher Ingenieure e. V., pp. 14-19, 04.2011.

[2] Carl Mahr Holding GmbH, "Verfahren und Vorrichtung zur Werkzeugvermessung" *DE Patent 10 2007 053 993 B4*, 08.2010.

[3] M. Büchner "Automatic Control for Lighting and Focussing in Green Vision", *NEMO-SpectroNet Collaboration Forum*, vol. 09, Jena, 12.2010.

[4] M. Büchner "Optische Messverfahren zur Hochgeschwindigkeitsprüfung von rotationssymmetrischen Präzisionwerkzeugen" *112th conference of the DGaO*, p. A23, Ilmenau, 06.2011.

[5] H. Hage, D. Ernst, "Präzisionsmessung", *Quality Engineering*, vol. 05, pp. 68-69, 1999.

[6] G. P. Israel, H. O. Sakman, "Elektronische Bildkorrektur", *Photonik*, vol. 01, 2007.

[7] H. Hengen, M. Pahdit, T. Paulus "Ein identifikationsbasierter Algorithmus zur geometrischen Verzeichnungskorrektur", *Image processing and machine vision*, vol. 1572, pp. 225-234, Stuttgart, 2000.

[8] G. Polte, K.-J. Rennert, G. Linß, "Korrektur von Abbildungsfehlern für optische Messverfahren", *Workshop "Flexible Montage"*, Ilmenau, 03.2010.

[9] N. Schuster, C. Maczeyzik, G. Gobsch, "Messung und Kompensation des Telezentriefehlers", *Photonik*, vol. 01, 2005.

[10] R. Schuhmann, T. Thöniß, "Telezentrische Systeme für die optische Meß- und Prüftechnik" *Technisches Messen 65*, vol. 04, pp. 131-136, 1998.

[11] S. Töpfer: "Automatisierte Antastung für die hochauflösende Geometriemessung mit CCD-Bildsensoren", *Dissertation,* pp. 57-74, Ilmenau, 2008

Author(s): Marco, Büchner, Mahr OKM GmbH, Carl-Zeiss-Promenade 10, 07745 Jena, Germany, +493641-642714, marco.buechner@mahr.de; Silvio Holder, Faculty of Mechanical Engineering, Department of Quality Assurance and Industrial Image Processing, University of Technology Ilmenau, Gustav-Kirchhoff-Platz 2, 98693 Ilmenau, Germany +493677-693937, silvio.holder@tu-ilmenau.de; Frank Richter, Mahr OKM GmbH, Carl-Zeiss-Promenade 10, 07745 Jena, Germany, +493641-642616, frank.richter@mahr.de; Dr.-Ing. Uwe, Nehse, Mahr OKM GmbH, Carl-Zeiss-Promenade 10, 07745 Jena, Germany, +493641-642831, uwe.nehse@mahr.de